

6-8-2015

Transient reflectance of photoexcited Cd_3As_2

Christopher P. Weber
Santa Clara University, cweber@scu.edu

Ernest Arushanov

Bryan S. Berggren

Tahereh Hosseini

Nikolai Kouklin

See next page for additional authors

Follow this and additional works at: <https://scholarcommons.scu.edu/physics>

 Part of the [Condensed Matter Physics Commons](#)

Recommended Citation

Weber, C. P., Arushanov, E., Berggren, B. S., Hosseini, T., Kouklin, N., & Nateprov, A. (2015). Transient reflectance of photoexcited Cd_3As_2 . *Applied Physics Letters*, 106(23), 231904. <https://doi.org/10.1063/1.4922528>

Copyright © 2015 American Institute of Physics Publishing. Reprinted with permission.

This Article is brought to you for free and open access by the College of Arts & Sciences at Scholar Commons. It has been accepted for inclusion in Physics by an authorized administrator of Scholar Commons. For more information, please contact rsroggin@scu.edu.

Authors

Christopher P. Weber, Ernest Arushanov, Bryan S. Berggren, Tahereh Hosseini, Nikolai Kouklin, and Alex Nateprov

Transient reflectance of photoexcited Cd_3As_2

C. P. Weber,^{1,a)} Ernest Arushanov,² Bryan S. Berggren,¹ Tahereh Hosseini,³ Nikolai Kouklin,³ and Alex Nateprov²

¹*Department of Physics, Santa Clara University, 500 El Camino Real, Santa Clara, California 95053-0315, USA*

²*Institute of Applied Physics, Academy of Sciences of Moldova, Academiei str. 5, MD 2028 Chisinau, Moldova*

³*Departments of Electrical Engineering and Computer Science, University of Wisconsin-Milwaukee, P.O. Box 413, Milwaukee, Wisconsin 53201, USA*

(Received 10 March 2015; accepted 3 June 2015; published online 11 June 2015)

We report ultrafast transient-grating measurements of crystals of the three-dimensional Dirac semimetal cadmium arsenide, Cd_3As_2 , at both room temperature and 80 K. After photoexcitation with 1.5-eV photons, charge-carriers relax by two processes, one of duration 500 fs and the other of duration 3.1 ps. By measuring the complex phase of the change in reflectance, we determine that the faster signal corresponds to a decrease in absorption, and the slower signal to a decrease in the light's phase velocity, at the probe energy. We attribute these signals to electrons' filling of phase space, first near the photon energy and later at lower energy. We attribute their decay to cooling by rapid emission of optical phonons, then slower emission of acoustic phonons. We also present evidence that both the electrons and the lattice are strongly heated. © 2015 AIP Publishing LLC.

[<http://dx.doi.org/10.1063/1.4922528>]

Cadmium arsenide, known for decades as an inverted-gap semiconductor, has recently been shown to be a three-dimensional Dirac semimetal.¹⁻⁴ These materials, with a massless Dirac dispersion throughout the bulk, are the 3D analogs of graphene, and Cd_3As_2 is foremost among them: stable, high-mobility, and nearly stoichiometric. It displays giant magnetoresistance,⁵ hosts topologically nontrivial Fermi-arc states on its surface,⁶ and is predicted to serve as a starting point from which to realize a Weyl semimetal, quantum spin Hall insulator, or axion insulator.^{1,7}

Ultrafast spectroscopy, which monitors changes in a sample's optical properties after excitation by a short laser pulse, has—in many materials—provided a time-resolved probe of basic carrier relaxation processes such as electron-electron and electron-phonon scattering and carrier diffusion. Calculations⁸ for Dirac and Weyl semimetals predict that photoexcited electrons will, anomalously, cool linearly with time once their energy drops below that of the lowest optical phonon. Nothing, however, is known of cadmium arsenide's ultrafast properties. Here, we use the transient-grating method, which measures both the magnitude and phase of the complex change of reflectance. Our measurements reveal two processes, distinct in lifetime and in phase, by which the sample's reflectance recovers after photoexcitation. Analysis of the signal's phase allows us to identify changes in both the real and the imaginary parts of the index of refraction, $n = n_r + in_i$. The fastest response, with a lifetime of 500 fs, is a reduction in the absorptive part, n_i , which we attribute to photoexcited electrons' filling of states near the excitation energy. The longer-lived response is an increase in n_r and arises from the filling of states at much lower energy. These observations reveal a two-stage cooling process, which we suggest may proceed first through optical phonons, then through acoustic.

We measured two samples of Cd_3As_2 . Sample 1 had well-defined crystal facets and measured a few millimeters in each dimension. It was grown by evaporation of material previously synthesized in Argon flow⁹ and was annealed at room-temperature for several decades. Such annealing is known to increase electron mobility and to decrease electron concentration.¹⁰ Indeed, Hall measurements on a sample of the same vintage give electron density $n = 6 \times 10^{17} \text{ cm}^{-3}$ (roughly independent of temperature), metallic resistivity,¹¹ and mobility $\mu = 8 \times 10^4 \text{ cm}^2/\text{V s}$ at 12 K. X-ray powder diffraction gives lattice parameters in agreement with previous reports.⁹

Sample 2 was grown in an Argon-purged chamber by CVD in the form of a platelet; the surface was microscopically flat and uniform. The ratio of the main Cd and As peaks seen in energy-dispersive X-ray spectroscopy corresponds to Cd_3As_2 , indicating proper stoichiometry. Though its transport was not unambiguously metallic,¹¹ in our experiment samples 1 and 2 behaved identically. This is consistent with the interpretation given below that our ultrafast signal arises from the dynamics of high-energy electrons.

We use the transient-grating method to measure the change, $\Delta r(t)$, in reflectance after photoexcitation. A pair of pump pulses interfere at the sample, exciting electrons and holes in a sinusoidal pattern. The sinusoidal variation in n caused by this excitation is the “grating.” Time-delayed probe pulses reflect and diffract off of the grating.

The experimental geometry is shown in Fig. 1. We use a diffractive-optic beamsplitter^{12,13} to generate the pair of pump pulses. As these pulses converge on the sample, they make angles $\pm\alpha$ with the surface normal, creating a grating of wavevector $q = (4\pi \sin \alpha)/\lambda$. (Here λ is the light's wavelength.)

Two probe pulses are incident on the sample at the same angles, $\pm\alpha$. The difference in their wavevectors equals q ; so, when each probe diffracts off of the grating, it is scattered to be collinear with the other probe.

^{a)}Electronic mail: cweber@scu.edu

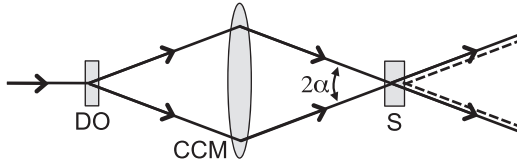


FIG. 1. Schematic diagram of the transient-grating experiment. For clarity, the mirror is shown as a lens, and beams reflected from the sample are shown as transmitted. A probe beam is focused onto a transmissive diffractive optic (DO) that directs most energy into the ± 1 orders. A concave mirror (CCM) focuses the two probes onto the sample (S), at an angle α from the normal. Diffracted beams (dashed) scatter through $\pm 2\alpha$, so that each diffracted probe is collinear with the opposite reflected probe. Pump beams (not shown) follow the same paths. However, pump beam paths are tipped slightly out of the page, and probe beams slightly into the page. Thus, the pumps are not collinear with the probes, nor are the reflected beams collinear with the incident ones.

This geometry allows for simple heterodyne detection^{12–14} of the diffracted probe: rather than providing a separate “local oscillator” beam, the reflected beam from one probe acts as a local oscillator for the diffracted beam from the other probe. If an incident probe has electric field E_0 , then the reflected and diffracted probe fields are, respectively,

$$\begin{aligned} E_r &= |r|e^{i\phi_r}E_0 + |\Delta r(t)|e^{i\phi_{\Delta r}}E_0, \\ E_d &= |d(t)|e^{i(\phi_{\Delta r} + m\phi_x)}E_0. \end{aligned} \quad (1)$$

Here, r is the complex reflectance, m is the order of diffraction, and ϕ_x is a geometric phase due to the grating’s spatial location. ϕ_x cannot be measured, but it can be changed controllably. Heterodyne detection of $|E_r + E_d|^2$ improves signal, and we suppress noise by modulation of ϕ_x and lock-in detection. The transient-grating signal is proportional to¹¹

$$|r||d(t)|\sin(\phi_r - \phi_{\Delta r} - m\phi_x). \quad (2)$$

Each measurement is repeated with the grating shifted by a quarter wavelength, giving the real and imaginary parts of $d(t)$. In the absence of measurable diffusion, as seen here, $d(t) \propto \Delta r(t)$.

The laser pulses have wavelength near 810 nm, duration 120 fs, repetition rate 80 MHz, and are focused to a spot of diameter 114 μm . The pump pulses have fluence f at the sample of 2.4–9.5 $\mu\text{J}/\text{cm}^2$; the probe pulses are a factor of 10 weaker. At 810 nm, Cd_3As_2 has index of refraction¹⁵ $n = 3.3 + 1.4i$, giving $\phi_r = 194^\circ$. The absorption length is of

order 45 nm, and the reflectivity is 35%; so, at our highest fluence, each pair of pump pulses photoexcites electrons and holes at a mean density of $n_{\text{ex}} \approx 5.7 \times 10^{18} \text{cm}^{-3}$. Measurements were taken at temperatures $T = 295 \text{ K}$ and 80 K, and one at 115 K.

Examples of the data obtained appear in Fig. 2. All of our data fit well to the form

$$\Delta r(t) = Ae^{i\theta_A}e^{-t/\tau_A} + Be^{i\theta_B}e^{-t/\tau_B} + Ce^{i\theta_C}. \quad (3)$$

The data’s three most salient features are each evident. First, the signal returns to equilibrium through two distinct decay processes, the first with $\tau_A = 500 \pm 35 \text{ fs}$ and the second with $\tau_B = 3.1 \pm 0.1 \text{ ps}$.¹⁶ Second, the two decay processes differ distinctly in complex phase. Finally, as shown in Fig. 3, the decays are insensitive to both q and f . Of these observations, the complex phase will play the key role in our identification, below, of the causes of the two decay processes.

In fact, the transient reflectance is even less sensitive to experimental conditions than Fig. 3 indicates. We varied the conditions—sample, T , f , m , and q —to measure 32 distinct $\Delta r(t)$ curves; we saw little variation in any of the fitting parameters of Eq. (3). The relative size of the two decay processes is constant, $A/B = 1.9 \pm 0.2$. The constant term increases from $C/B = 0.05$ at 80 K to 0.10 at 295 K, but always remains small. We attribute the C term to lattice heating, for which we present qualitative evidence in the supplementary material.¹¹

Transient-grating experiments are often used to measure the diffusivity D of photoexcited species. In the presence of diffusion, the diffracted signal $d(t)$ decays faster than $\Delta r(t)$ because carriers diffuse from the grating’s peaks to its troughs. This effect is stronger at higher q , because the peak-to-trough distance is shorter. However, Fig. 3(d) shows that τ_B is independent of q , consistent with $D = 0$. We caution against assigning too much weight to this negative result. The sloped line in Fig. 3(d) shows that our data exclude only $D > 60 \text{ cm}^2/\text{s}$ —a distinctly high upper bound. So, the carriers likely do diffuse, but relax so quickly that they do not diffuse through an appreciable fraction of the grating’s wavelength.¹⁷ The situation for τ_A is similar: Fig. 3(c).

Our typical measurement, of $m = +1$, is not sensitive to the multiplication of Eq. (3) by an overall phase. However, by additionally measuring $m = -1$, it is possible to determine the absolute phase¹⁴ of Δr . We have done several such

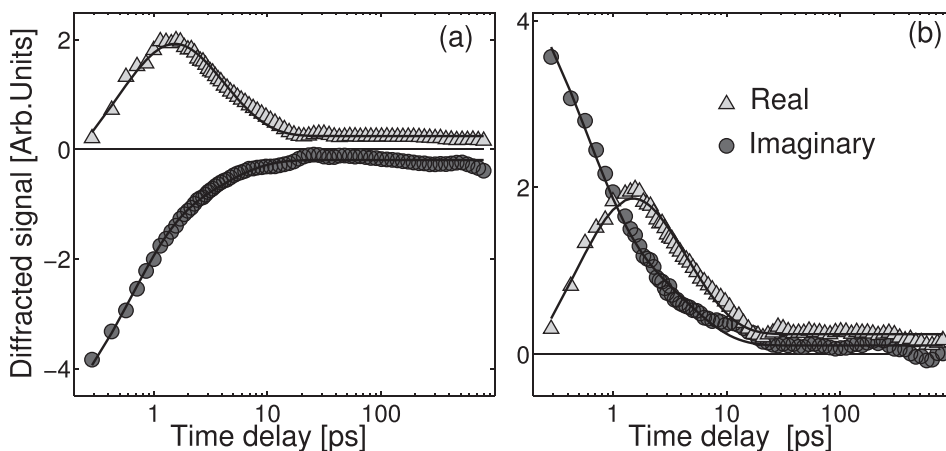


FIG. 2. Typical transient-grating data (semilog time). All three components of the signal are clearly visible. Real part, triangles; imaginary part, circles; lines are fits to Eq. (3). $T = 295 \text{ K}$, $q = 3.14 \mu\text{m}^{-1}$, $f = 7.8 \mu\text{J}/\text{cm}^2$. (a) and (b) are $m = +1$ and -1 diffracted orders, respectively.

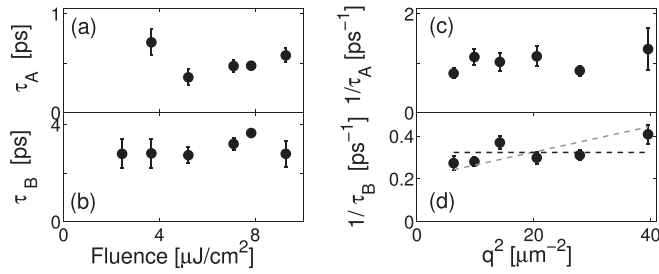


FIG. 3. (a) and (b). τ_A and τ_B are roughly constant vs. pump fluence. (c) and (d). $1/\tau_A$ and $1/\tau_B$ are roughly constant vs. q^2 . τ_B is consistent with diffusion coefficients from $D=0$ (horizontal line) to $D=60 \text{ cm}^2/\text{s}$ (sloped line).

measurements on each sample; one appears in Fig. 2(b). We can then calculate¹¹

$$\phi_{\Delta r}^A = \frac{\theta_A^{(-)} - \theta_A^{(+)} - \pi}{2} + \phi_r, \quad (4)$$

and similarly for the signal's B and C components. Though the half-angle in Eq. (4) can take two values differing by 180° , this ambiguity is easily resolved. The photoinduced change in reflectivity is $\Delta R = 2|r||\Delta r(t)| \cos(\phi_r - \phi_{\Delta r})$; we measure $\Delta R(t)$ and choose the angles $\phi_{\Delta r}$ to reproduce its sign, shown in Figs. 4(a) and 4(b).

We now use these angles to determine the photoinduced change in n . The reflectance changes after photoexcitation by $\Delta r(t) = [-2/(1+n)^2]\Delta n(t)$. For cadmium arsenide, the bracketed factor has argument 143° , so $\phi_{\Delta n} = \phi_{\Delta r} - 143^\circ$. We obtain, finally, $\phi_{\Delta n}^A = -80^\circ$, $\phi_{\Delta n}^B = -8^\circ$, and $\phi_{\Delta n}^C = -25^\circ$.

This result is surprisingly simple. The signal's faster component results from a negative Δn_i —a reduction in absorption—and the slower from a positive Δn_r —a decrease in the light's phase velocity. The calculated $\Delta n(t)$ appears in Fig. 4(c). For Cd_3As_2 , both the real and imaginary parts of Δn appear in ΔR , and they may be distinguished by the time-scales of their decays.

The key questions in interpreting these two decay processes are what has been excited, and by what means it relaxes. Our excitation energy $\varepsilon_p = 1.5 \text{ eV}$ is well beyond the region of cadmium arsenide's Dirac-like dispersion, and,

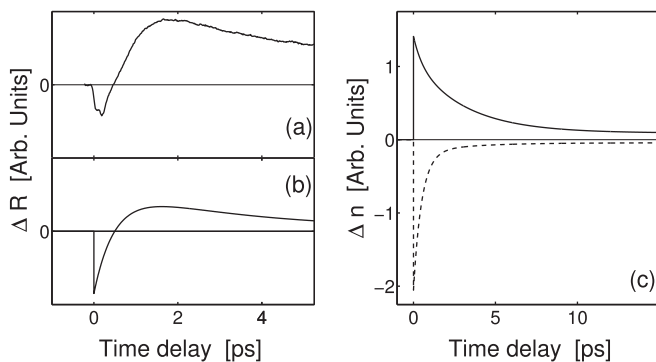


FIG. 4. (a) Typical transient change in reflectivity, $\Delta R(t)$, measured. (b) $\Delta R(t)$, calculated from our mean fit parameters. The sign of each component is chosen to match the shape of the measured curve. (c) Transient change, Δn , in index of refraction calculated from our mean fit parameters. Imaginary part (dashed) accounts for most of the fast decay. Real part (solid) accounts for most of the slow decay and the constant term.

though optical transitions near 1.5 eV are believed to occur at the Γ point,¹⁵ transitions are allowed between electrons and holes of several different bands. Cadmium arsenide's large unit cell hosts over 200 phonon branches; infrared and Raman measurements detect a few dozen,^{18–21} with energies from 3.2 meV to 49 meV (The deficit of detected branches is attributed to a weak polarizability.²¹). Considering the abundance of excited states and relaxation pathways available, we cannot hope to identify precise processes of excitation or relaxation. Nonetheless, the optical signal's phase constrains our interpretation significantly.

Photoexcitation changes a sample's reflectance by changing its frequency-dependent absorption coefficient. Leaving aside the possibility of changes to the band structure, it does so either by occupying excited states or by changing the free carriers' absorption. Our experiment's probe photons have the same energy ε_p as those of the pump. Therefore, excited electrons fill phase-space effectively, reducing absorption at ε_p , and causing the negative Δn_i observed in our fast decay process.

This picture remains valid even as electrons scatter away from their initial excited energy ε_e .²² Carrier-carrier scattering gradually creates a thermal distribution of electrons at elevated temperature. If this process is fast compared to the carriers' energy loss, their mean energy remains nearly ε_e , and they occupy states both below and above ε_e . Such a distribution results in $\Delta n_i < 0$, just as does the conceptually simpler case of phase-space filling exactly at ε_e .

Our signal's slower component has $\Delta n_r > 0$, which—according to the Kramers-Kronig relation—must result either from increased absorption at $\varepsilon > \varepsilon_p$ or from decreased absorption at $\varepsilon < \varepsilon_p$. We can eliminate the former as the cause of our signal. If absorption increases at all, it should do so at low frequency due to enhanced free-carrier (intra-band) conductivity; this would cause a negative Δn_r that we do not observe. On the other hand, there is a straightforward mechanism for decreased absorption at $\varepsilon < \varepsilon_p$: as electrons and holes lose their excess energy, they fill phase space at progressively lower energies. Kramers-Kronig analysis using a simplified density of states suggests that, by the time $\Delta n(\varepsilon_p)$ becomes mostly real, the carriers' mean energy should be $\varepsilon_e/2$ or less; our data show that cooling of this magnitude occurs within 500 fs . We attribute this cooling to phonons rather than to carrier-carrier scattering, since there are too few cool, background electrons compared to the hot, photoexcited ones (an order of magnitude fewer for sample 1 and at our highest fluence).

The subsequent dynamics of Δn_r indicate that once carriers reach low energy, their relaxation slows to give $\tau_B = 3.1 \text{ ps}$. Possibly cooling slows when the carriers' excess energy falls below that of the lowest optical phonon, as occurs in graphene^{23,24} and as recently predicted for Weyl and 3D Dirac semimetals.⁸ However, for Cd_3As_2 , this energy is just 15 meV .²¹ Other possible relaxation processes include electron-impurity scattering or electron-electron scattering with plasmon emission. However, we suggest that after the initial 500-fs cooling the carriers and optical phonons have equilibrated; further cooling requires the slower emission of acoustic phonons. This picture fits the measured time-scale: electron-lattice cooling in bismuth, a semimetal, occurs in 5 ps .²⁵

We may gain insight into the two decay processes we observe in cadmium arsenide by considering another Dirac semimetal, graphene. Photoexcitation of graphene initially produces electrons and holes with separate chemical potentials.²⁶ Within the pulse duration, these carriers partially equilibrate with optical phonons;²⁷ they then quickly occupy the Dirac cone and enhance the intraband conductivity,²⁸ and recombine in less than a picosecond.²⁶ The chemical potential reverts to its original level, but—because carriers are still hot—they continue to occupy high-energy states, filling phase-space and reducing optical absorption.²⁹ These hot carriers finally relax *via* optical, then acoustic, phonons.^{23,24}

Our measurements indicate that some of the same processes occur in cadmium arsenide, but possibly not all. We do not know whether carriers relax into the Dirac cone, but the weakness of cadmium arsenide's photoluminescence³⁰ suggests that many do. We also cannot conclude that, as in graphene, photoexcitation produces electrons and holes with separate chemical potentials; time-resolved photoemission and THz could more directly detect changes in carrier population and conductivity.

In conclusion, we have shown that after photoexcitation, cadmium arsenide relaxes in two distinct stages, irrespective of sample, fluence, and temperature. First, carriers fill phase-space at the pump energy, but relax within 500 fs to lower energy. These low-energy carriers relax further with a timescale of 3.1 ps; the lattice finally reaches high temperature. This result may guide further ultrafast measurements on Cd₃As₂ and other Dirac and Weyl semimetals.

This work was supported by the National Science Foundation Grant No. DMR-1105553.

¹Z. Wang, H. Weng, Q. Wu, X. Dai, and Z. Fang, *Phys. Rev. B* **88**(12), 125427 (2013).

²M. Neupane, S.-Y. Xu, R. Sankar, N. Alidoust, G. Bian, C. Liu, I. Belopolski, T.-R. Chang, H.-T. Jeng, H. Lin, A. Bansil, F.-C. Chou, and M. Z. Hasan, *Nat. Commun.* **5**, 3786 (2014).

³Z. K. Liu, J. Jiang, B. Zhou, Z. J. Wang, Y. Zhang, H. M. Weng, D. Prabhakaran, S. K. Mo, H. Peng, P. Dudin, T. Kim, M. Hoesch, Z. Fang, X. Dai, Z. X. Shen, D. L. Feng, Z. Hussain, and Y. L. Chen, *Nat. Mater.* **13**(7), 677 (2014).

⁴S. Borisenko, Q. Gibson, D. Evtushinsky, V. Zabolotnyy, B. Büchner, and R. J. Cava, *Phys. Rev. Lett.* **113**(2), 027603 (2014).

⁵T. Liang, Q. Gibson, M. N. Ali, M. Liu, R. J. Cava, and N. P. Ong, *Nat. Mater.* **14**, 280 (2015).

⁶H. Yi, Z. Wang, C. Chen, Y. Shi, Y. Feng, A. Liang, Z. Xie, S. He, J. He, Y. Peng, X. Liu, Y. Liu, L. Zhao, G. Liu, X. Dong, J. Zhang, M. Nakatake, M. Arita, K. Shimada, H. Namatame, M. Taniguchi, Z. Xu, C. Chen, X. Dai, Z. Fang, and X. J. Zhou, *Sci. Rep.* **4**, 6106 (2014).

⁷X. Wan, A. M. Turner, A. Vishwanath, and S. Y. Savrasov, *Phys. Rev. B* **83**(20), 205101 (2011).

⁸R. Lundgren and G. A. Fiete, preprint [arXiv:1502.07700](https://arxiv.org/abs/1502.07700) (2015).

⁹E. K. Arushanov, *Prog. Cryst. Growth Charact.* **3**(2–3), 211 (1981).

¹⁰A. Rambo and M. J. Aubin, *Can. J. Phys.* **57**, 2093 (1979).

¹¹See supplementary material at <http://dx.doi.org/10.1063/1.4922528> for the samples' transport properties, additional description of the transient grating, and a discussion of optical heating of the samples.

¹²G. D. Goodno, G. Dadusc, and R. J. D. Miller, *J. Opt. Soc. Am. B* **15**(6), 1791 (1998).

¹³A. A. Maznev, K. A. Nelson, and T. A. Rogers, *Opt. Lett.* **23**(16), 1319 (1998).

¹⁴N. Gedik and J. Orenstein, *Opt. Lett.* **29**(18), 2109 (2004).

¹⁵K. Karnicka-Moscicka, A. Kisiel, and L. Źdanowicz, *Solid State Commun.* **44**(3), 373 (1982).

¹⁶Errors and error-bars are standard deviation of the mean.

¹⁷The lack of measurable diffusion is perhaps to be expected. Photoexcited electrons and holes must move together to preserve local charge neutrality, resulting in ambipolar diffusion. In an *n*-type sample, the ambipolar diffusivity nearly equals the holes' diffusivity, which is likely much less than the electrons'.

¹⁸M. J. Gelten and C. M. van Es, *Phys. Narrow Gap Semicond.* **152**, 167 (1982).

¹⁹H. M. A. Schleijsen, M. von Ortenberg, M. J. Gelten, and F. A. P. Blom, *Int. J. Infrared Millim. Waves* **5**(2), 171 (1984).

²⁰S. Jandl, S. Desgreniers, C. Carlone, and M. Aubin, *J. Raman Spectrosc.* **15**(2), 137 (1984).

²¹D. Houde, S. Jandl, M. Banville, and M. Aubin, *Solid State Commun.* **57**(4), 247 (1986).

²²Note that electronic energy of ϵ_c corresponds to optical transitions at ϵ_p .

²³R. Bistritzer and A. H. MacDonald, *Phys. Rev. Lett.* **102**(20), 206410 (2009).

²⁴J. H. Strait, H. Wang, S. Shivaraman, V. Shields, M. Spencer, and F. Rana, *Nano Lett.* **11**(11), 4902 (2011).

²⁵Y. M. Sheu, Y. J. Chien, C. Uher, S. Fahy, and D. A. Reis, *Phys. Rev. B* **87**, 075429 (2013).

²⁶S. Gilbertson, G. L. Dakovski, T. Durakiewicz, J.-X. Zhu, K. M. Dani, A. D. Mohite, A. Dattelbaum, and G. Rodriguez, *J. Phys. Chem. Lett.* **3**(1), 64 (2012).

²⁷C. H. Lui, K. F. Mak, J. Shan, and T. F. Heinz, *Phys. Rev. Lett.* **105**(12), 127404 (2010).

²⁸K. M. Dani, J. Lee, R. Sharma, A. D. Mohite, C. M. Galande, P. M. Ajayan, A. M. Dattelbaum, H. Htoon, A. J. Taylor, and R. P. Prasankumar, *Phys. Rev. B* **86**(12), 125403 (2012).

²⁹D. Sun, Z. K. Wu, C. Divin, X. B. Li, C. Berger, W. A. de Heer, P. N. First, and T. B. Norris, *Phys. Rev. Lett.* **101**(15), 157402 (2008).

³⁰M. O'Neil, J. Marohn, and G. McLendon, *J. Phys. Chem.* **94**, 4356 (1990).